Membrane binding strongly affects dopamine reactivity induced by Cu-prion and Cu-Aβ peptides. A ternary Cu-Aβ-prion peptide complex is stabilized and solubilized in SDS micelles

Chiara Bacchella,[a] Stefania Nicolis,[a] Simone Dell'Acqua,[a] Enrico Rizzarelli,[b] Enrico Monzani,*[a] Luigi Casella*[a]

[a] Dipartimento di Chimica, Università di Pavia, Via Taramelli 12, 27100 Pavia, Italy

[b] Istituto di Biostrutture e Bioimmagini, Consiglio Nazionale delle Ricerche, Via P. Gaifami 18, 95125 Catania, Italy

Prion peptides • Copper complexes • Dopamine • Oxidative stress • Post-translational protein modification

ABSTRACT: The combination between dyshomeostatic levels of catecholamine neurotransmitters and redox active metals such as copper and iron exacerbates the oxidative stress condition that typically affects neurodegenerative diseases. We report a comparative study of the oxidative reactivity of copper complexes with amyloid-β ($A\beta_{40}$) and the prion peptide fragment 76-114 (PrP_{76-114}), containing the high affinity binding site, towards dopamine and 4-methylcatechol, in aqueous buffer and in SDS micelles, as a model membrane environment. The competitive oxidative and covalent modifications undergone by the peptides were also evaluated. The high binding affinity of [Cu-peptide] to micelles and lipid membranes leads to a strong reduction ($A\beta_{40}$) and quenching (PrP_{76-114}) of the oxidative efficiency of the binary complexes and to a stabilization and redox silencing of the ternary complex Cu^{II}-$A\beta_{40}$-PrP_{76-114}, which is highly reactive in solution. The results improve our understanding of pathological and protective effects associated with these complexes, depending on the physiological environment.

INTRODUCTION

The dyshomeostasis of neurometals, in particular iron, zinc, copper and manganese, in various brain areas contributes to the pathogenesis of several neurodegenerative diseases, including Alzheimer's disease (AD), prion diseases, and Parkinson's disease (PD).[1-3] Among the possible effects ascribable to metal ions are the impairment of normal brain functions, such as neurotransmitter synthesis[4] and neural information processing,[5-7] and the induction of conformational changes and/or aggregation of various disease-related proteins, including α-synuclein (αSyn) in PD, β-amyloid (Aβ) and tau in AD, and prion protein (PrP) in prion diseases.[8] There is an emerging link between the membrane-anchored form of cellular PrP and amyloid proteins, in their monomeric or oligomeric forms, as PrP appears to act as the binding receptor for αSyn,[9] Aβ,[10] and tau.[11] This interaction has been proposed as the basic mechanism promoting neuronal spreading of neurotoxic protein aggregates and the related pathologies.[12] It is interesting that a main PrP region involved in the binding of β-rich peptides, including Aβ,[13] (termed CC2 and comprising residues 94-110) partially overlaps with the high-affinity copper(II) binding site,[14] as shown schematically in Chart 1, although it is not known whether copper participates in this interaction. As a matter of fact, Aβ appears to interrupt copper-mediated PrP interaction with N-methyl-D-aspartate receptors.[15] In addition, cellular PrP is proteolyzed in a similar way to amyloid precursor protein, generating distinct truncated forms, which are found *in vivo*,[16] and this process is supported by copper(II) induced reactive oxygen species (ROS).[17] Copper redox reactivity can be responsible for damaging other neuronal peptides and proteins, as shown by the oxidative effects extensively claimed in the literature.[7,18] On the other hand, both PD and AD diseased brains bear marks of massive molecular oxidative stress,[19] and dysregulated copper is certainly an important player in these pathologies.

Although several reports describe protective effects by Aβ and other neuronal proteins against copper (and iron) generated ROS,[20] it should be pointed out that decreased ROS formation is due to the sacrificial oxidation and fragmentation of the proteins, as the Cu-bound forms of the proteins bear an increase of oxidative reactivity compared to "free" copper. In addition, as we have recently shown, the presence of dopamine (DA) and other catechols exacerbates the effects of Cu redox cycling and Cu-induced oxidative stress in the presence of Aβ peptides[21] and the PrP fragments containing N-terminal αSyn the copper-catalyzed oxidative reactions are reduced.[23]

We have systematically found that in addition to promoting Cu redox reactivity, the catechol-derived quinones are able to modify covalently the peptide chains at nucleophilic residues. The reference to DA is thus important because its contribution may not be limited to the promotion of oxidative stress. Indeed, although the role of DA in αSyn aggregation and Lewy bodies has been early recognized,[24] the effect was only ascribed to its redox activity or protein binding. While coupling of αSyn with ubiquitin in Lewy bodies and other αSyn pathologies could be recognized with anti-ubiquitin antibodies,[24,25] suitable antibodies for detection of quinone modified proteins were never developed. Besides promoting αSyn aggregation, DA has been recently associated with PrP aggregation and oxidative cleavage,[26] and it is very likely that also in this case quinone modification of the protein occurs in the process, as suggested by our *in vitro* study.[22] More generally, alterations in DA metabolism affect brain areas different from the *substantia nigra*, where PD is initially localized, such as the regions typically affected in AD.[27]

Dopamine has been recently proposed as a modulator of Aβ aggregation and toxicity through covalent modification of the peptide.[28] The role of DA as a general source of protein posttranslational modification in neurodegenerative diseases has been recently reviewed.[29] As for the specificity of copper, it should be noted that noradrenergic neurons in *locus coeruleus*, which is affected both in PD and AD, contain much more mobilized and potentially toxic copper with respect to *substantia nigra* neurons.[30]

The analysis of the effects of Cu induced oxidative stress in the presence neuronal peptides and catecholamines is incomplete if it remains confined in the aqueous milieu. Both αSyn, Aβ and PrP strongly interact with membranes and often this interaction bears significant conformational changes in the peptides.[31] Membrane interaction is expected to affect also the redox reactivity of the metal-peptide complex and, in fact, we have recently shown that in the presence of SDS as a model membrane, redox cycling of the Cu complex with N-terminal αSyn peptide is completely quenched.[23c]

Regarding the copper binding details, the (high affinity) Cu^{II} binding site in PrP is located in the central portion of the ~230 amino acid sequence, whereas in the case of Aβ the Cu binding site is in the N-terminal portion. As shown schematically in Chart 1, the Cu^{II} ligands are, for the major forms present in solution, two His and two N(amide) donors in the case of PrP,[14] and two His and the N-terminal NH_2 and C=O groups of Asp1 in the case of Aβ.[32] Whereas Cu^{I} in PrP peptides is bound to two Met residues and H111 outside the octarepeats,[33] in Aβ it binds to two of the three residues His6, His13 and His14 in a linear, two-coordinate arrangement [34] (Chart 1). The main aim of this paper is then to show that the presence of SDS micelles has strong impact on catechol oxidation and peptide modification promoted by the Cu^{II} complexes with the PrP fragments $PrP_{106-114}$ and PrP_{76-114}, and with Aβ peptides $Aβ_{16}$, $Aβ_{28}$, and $Aβ_{40}$. SDS is advantageous with respect to more complex lipid bilayers because it allows an easier separation of peptide fragments and analysis of their modifications.

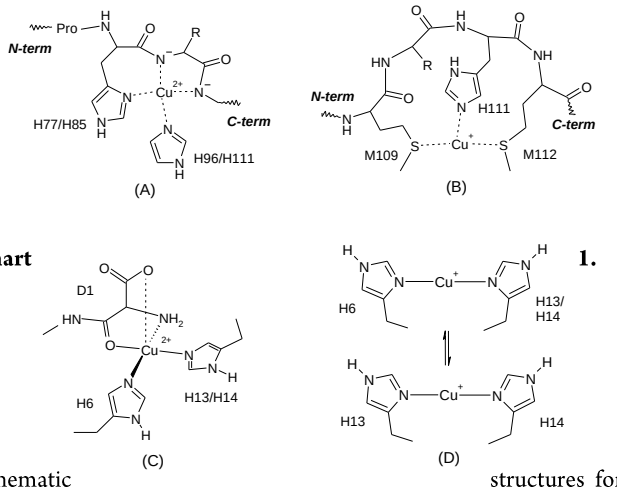

Chart 1. Schematic structures for the copper(II) and copper(I) complexes of PrP and Aβ peptides (major forms present in solution at physiological pH).

RESULTS AND DISCUSSION

Interaction of Cu-PrP and Cu-Aβ Complexes with SDS Micelles. The anionic surfactant SDS is used in this investigation because the negative surface charge and high affinity to hydrophobic domains of the micelles formed above the critical concentration (about 9 mM) represent a useful model of biological membranes. Human PrP contains two distinct domains, a long unstructured N-terminus (about 100 residues) containing the octarepeat (PHGGGWGQ) motifs, and a globular, mostly helical, C-terminus.[35] The CD spectra of free and Cu^{II}-bound PrP_{76-114} fragment (1:1 ratio) in buffer solution show typical features of unstructured peptides and very modest changes in the presence of SDS (Figure S1 and S2). The spectrum remains unchanged for Cu^{I}-PrP_{76-114} in SDS (Figure 1A). Similar results were obtained previously with larger PrP peptide fragments, like 91-115, adjacent to the α-helix structuring hydrophobic region comprising residues 115-127, in the presence of copper(II).[36]

The situation is different for Aβ peptides, because in this case, binding to SDS micelles involves partial structuring to α-helix, as shown in Figure 1B and 1C for $Aβ_{28}$ and $Aβ_{40}$, respectively. The smaller peptide $Aβ_{16}$ is essentially unstructured in aqueous solution but becomes also partially structured in SDS (Figure S3). It is known that in SDS micelles $Aβ_{40}$ adopts a helix-loop-helix structure defined by the two α-helices formed by residues 15-24 and 29-35.[37,38] The CD profiles exhibited by $Aβ_{28}$ and $Aβ_{40}$ peptides are similar, with the two minima around 208 and 222 nm. However, as expected, the CD intensity is larger for the longer peptide, since $Aβ_{28}$ only contains the first of the two helices. The extended structure of $Aβ_{40}$ C-terminal in the membrane mimicking environment makes it a potential membrane spanning helix, and could explain the membrane channel properties of Aβ.[18g,39] It is interesting to note that the CD spectra of the Cu^{I} and Cu^{II} complexes of $Aβ_{28}$ and $Aβ_{40}$ fairly overlap with those of the corresponding free peptides. This indicates that the structural arrangements in the N-terminal region of the peptides around the metal ions (Chart 1) does not seem to affect the α-helical structuring tendency of the hydrophobic portion inside the

membrane. As hypothesized before,[37] it is thus likely that the polar N-terminal fragment of Cu-bound Aβ peptides remains essentially confined in the aqueous *medium* outside the SDS micelles. This is confirmed by the finding that the binding constant of $A\beta_{40}$ for Cu^{II} is the same in the absence and presence of SDS micelles.[37,40]

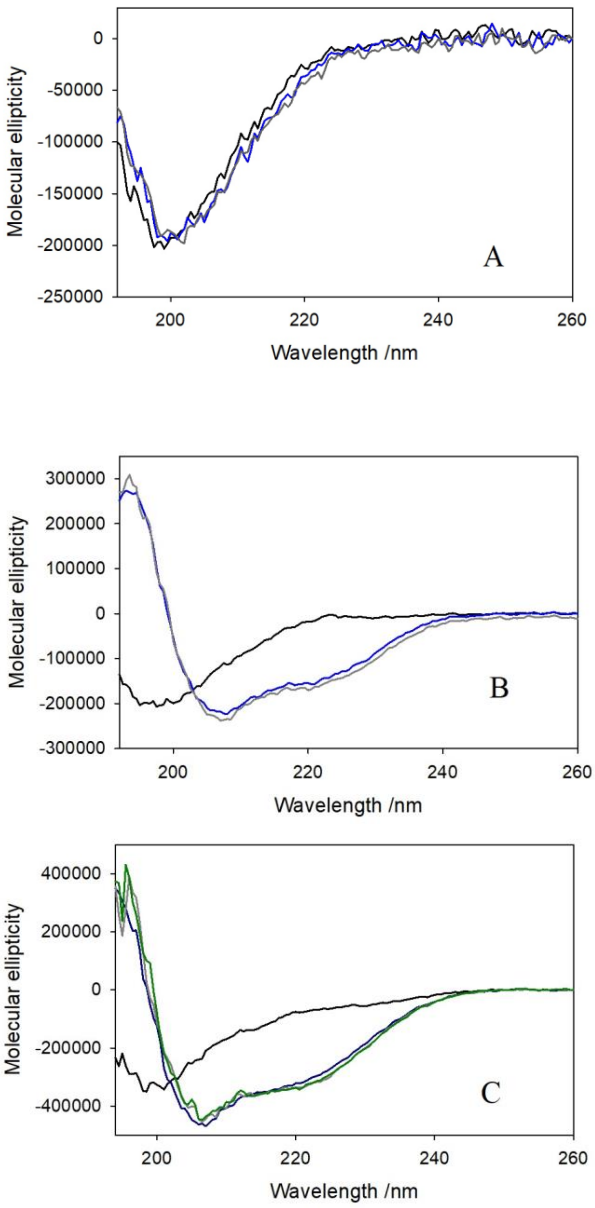

Figure 1. Far-UV CD spectra recorded in 5 mM phosphate buffer solution pH 7.4 of: (A) $PrP_{76\text{-}114}$ (5.5 μM), and (B) $A\beta_{28}$ (5.5 μM) (black traces), and after the addition of 20 mM SDS (blue traces) and Cu^{I} (5 μM) (grey traces). Copper(I) was generated *in situ* by reaction of copper(II) nitrate (5 μM) and hydroxylamine (10 μM) anaerobically (cell path 1 cm). Figure C shows CD spectra of $A\beta_{40}$ (4.4 μM), dissolved in water containing 0.6 mM NH_3, and recorded in 5 mM phosphate buffer solution pH 7.4 (black trace), and after the addition of 16 mM SDS (blue trace), Cu^{I} (4 μM) (grey trace) or Cu^{II} (green trace).

Oxidative Reactivity of Cu-PrP and Cu-Aβ Complexes in Solution and Bound to SDS Micelles. We have recently reported that binding of copper(II) to $PrP_{76\text{-}114}$, containing the high affinity binding site of prion protein, produces a marked increase in the catalytic oxidation capacity of the complex towards DA and 4-methylcatechol (MC) with respect to free Cu^{II} (we refer here to "free" Cu^{II} for simplicity, whereas in the reaction conditions it is indeed a Cu^{II}-catecholato complex).[22]

When these experiments are carried out in buffer solution at pH 7.4 in the presence of SDS micelles, a completely reversed trend is observed. While the reactivity of free copper(II) remains unaltered, that of Cu^{II}-$PrP_{76\text{-}114}$ is almost totally quenched, as shown in Figure 2 for MC (complete quenching occurs at higher peptide:Cu^{II} molar ratio). In this experiment, the molar ratio between Cu^{II} and $PrP_{76\text{-}114}$ is 1:2; when this ratio is decreased to 1:1, the reactivity is also quenched initially, but then slowly takes place (Figure 2).

The kinetic traces in these figures monitor the absorption of 4-methylquinone (MQ) at 401 nm with time in the initial phase of the reaction. At longer time, as MQ appreciably accumulates in solution, it undergoes a Michael addition by unreacted MC, and subsequently further reactions, resulting in further increase in absorption and red shift of the broad UV band.[21b] The trend is confirmed with the oxidation of DA (Figure 3), where the product monitored in the initial phase is dopaminochrome.[22,41] The reactivity of the catecholamine is lower than that of MC but it gives rise to a more complex mixture of oligomeric products.[41]

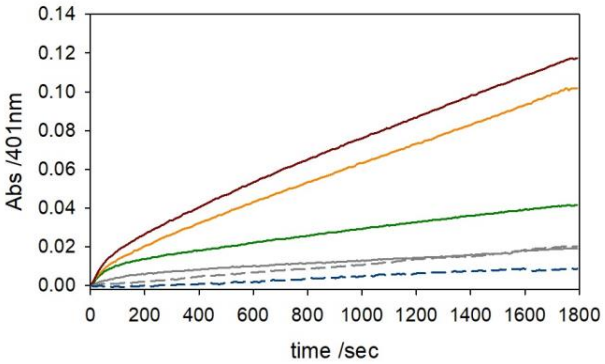

Figure 2. Kinetic profile of MC (3 mM) oxidation with time in 50 mM HEPES buffer solution at pH 7.4 and 20 °C in the presence of Cu^{II} (25 μM) without SDS (green trace), and upon the addition of 1 equiv. $PrP_{76\text{-}114}$ (25 μM) in the absence (orange)/presence (dashed grey trace) of SDS (20 mM), and 2 equiv. of peptide (50 μM) in absence (brown)/presence (dashed blue trace) of micelles.

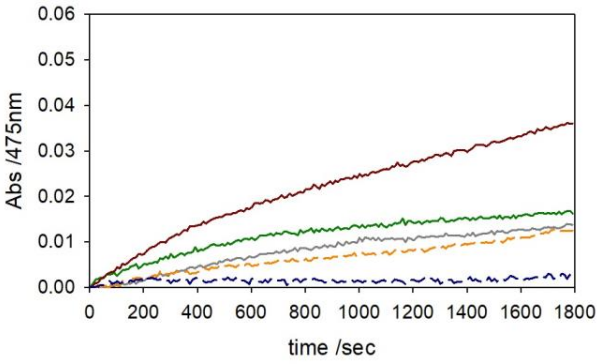

Figure 3. Kinetic profiles of DA (3 mM) oxidation with time in 50 mM HEPES buffer solution at pH 7.4 and 20 °C in the presence of

Cu^{II} (25 μM) without SDS (green trace) and with SDS (20 mM) (dashed orange trace), and in the presence of Cu^{II} (25 μM) and PrP_{76-114} (50 μM) without SDS (brown) and with SDS (20 mM) (dashed blue trace). DA autoxidation is also shown (grey trace).

The quenching of reactivity observed in SDS is due to the fact that upon reduction of copper(II), the Cu^{I}-PrP_{76-114} species trapped in the membrane is unreactive to dioxygen. This is confirmed by experiments carried out starting from the anaerobically prepared Cu^{I}-PrP_{76-114} complex (1:2 ratio as above) and then exposing the solution containing the catechol to air. Unlike "free" Cu^{I}, the Cu^{I}-peptide complex is completely unreactive to dioxygen (Figure 4).

The situation highlighted for Cu-PrP_{76-114} is therefore similar to the behavior of the copper complex with N-terminal αSyn in SDS,[23c] suggesting that the membrane environment has a protecting effect towards the redox reactivity of the Cu-peptide complex. With the shorter peptide $PrP_{106-114}$, the oxidation capacity of the Cu^{II}-$PrP_{106-114}$ complex is reduced,[22] however the reactivity against MC is not completely quenched in SDS micelles at the Cu^{II}/$PrP_{106-114}$ 1:2 molar ratio (Figure S4), due to incomplete copper(II) complexation by the shorter peptide.[22] In fact, complete quenching of the reactivity occurs at much higher $PrP_{106-114}$ concentration (Figure S5). It is interesting that when the experiment with $PrP_{106-114}$ is carried out preforming the Cu^{I}-peptide complex anaerobically, and then exposing the solution with MC to air, the reaction is almost totally quenched for a significant time span, but then MC oxidation starts abruptly, probably because the peptide undergoes extensive oxidation (Figure S6). The low reactivity of Cu^{II}-$PrP_{106-114}$ towards DA[22] is obviously also further depressed in SDS micelles (Figure S7). Finally, as the longer PrP peptide fragment PrP_{76-114} can bind more than one copper(II) ion, we checked whether the quenching of Cu reactivity in SDS could be maintained at a Cu/PrP_{76-114} 2:1 molar ratio. The Cu_2-PrP_{76-114} complex is indeed more reactive than its 1:1 homologue in aqueous medium, and its reactivity is only reduced, but not quenched in SDS (Figure S8).

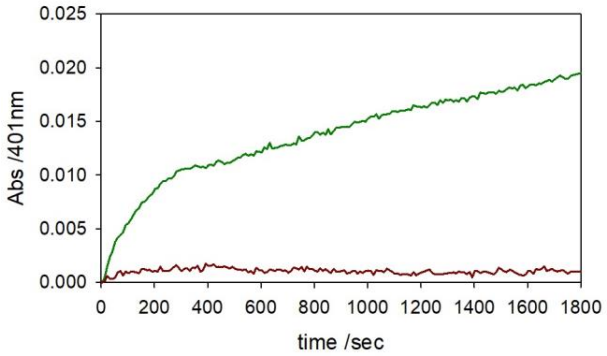

Figure 4. Kinetic profile of MC (3 mM) oxidation with time in 50 mM HEPES buffer solution at pH 7.4 and 20 °C containing SDS (20 mM) and in the presence of Cu^{I} (25 μM) alone (green trace) or Cu^{I} (25 μM) and PrP_{76-114} (50 μM) (brown trace). Copper(I) was generated *in situ* by reaction of copper(II) nitrate (25 μM) and ascorbate (50 μM) anaerobically prior to exposure of the solution to air.

When the experiments of catechol oxidation in aqueous solution and in membrane-like environment were performed with Cu-Aβ peptide complexes, a different behavior is observed. As it was shown previously, Cu^{II}-$Aβ_{16}$ and Cu^{II}-$Aβ_{28}$ complexes are very reactive against catechols in aqueous buffer at physiological pH.[21b] The presence of SDS micelles in these cases does not quench the reaction, but only partially reduces the catechol oxidation rate, as shown for MC and DA (Figure 5) in the case of Cu^{II}-$Aβ_{28}$. Thus, here the reduced copper complex is still reactive to dioxygen and allows redox cycling and catechol oxidation. This was confirmed by separate experiments where, as above, the reaction was started from preformed Cu^{I}-$Aβ_{28}$ complex under anaerobic conditions and subsequently exposing the solution to air (Figure S9). The reactivity of Cu^{II}-$Aβ_{16}$ complex in SDS is similar and the corresponding experiments are shown in Figure S10, S11, and S12.

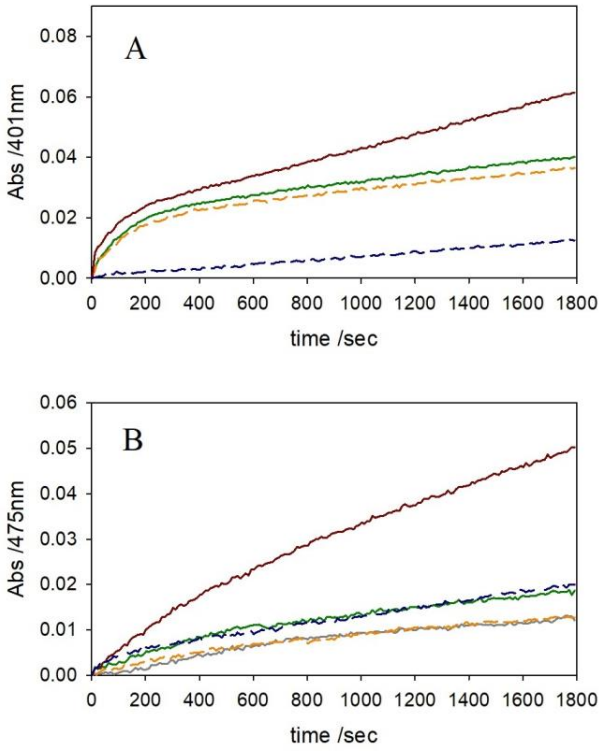

Figure 5. Kinetic profile of: (A) MC (3 mM) and (B) DA (3 mM) oxidation with time in 50 mM HEPES buffer solution at pH 7.4 and 20 °C in the presence of Cu^{II} (25 μM) without SDS (green trace) and with SDS (20 mM) (dashed orange trace), and in the presence of Cu^{II} (25 μM) and $Aβ_{28}$ (50 μM) without SDS (brown) and with SDS (20 mM) (dashed blue trace). DA autoxidation is shown as grey trace.

We did not investigate previously the reactivity of Cu^{II} bound to Aβ peptides longer than 1-28 because of their tendency to undergo aggregation in solution. However, the length of the peptide is important when interaction with membranes is considered and we thus report here the behavior of Cu-$Aβ_{40}$ complexes in the catechol oxidation reaction. To the end of reducing the rate of peptide aggregation in the time interval needed to perform reliable catalytic oxidation experiments with MC and DA, we found useful to add a small amount of ammonia to the buffer solution, since it is known that in these conditions the aggregation rate is significantly reduced at room temperature.[42] The small amount of ammonia added in the buffer has no influence on the reactivity of the complex. The reactivity pattern of Cu-$Aβ_{40}$ towards MC and DA is similar to that of complexes with smaller Aβ peptides (Figure S13 and S14), which

is expected, as the N-terminal Cu-binding portion remains outside of the membrane (Scheme 1).

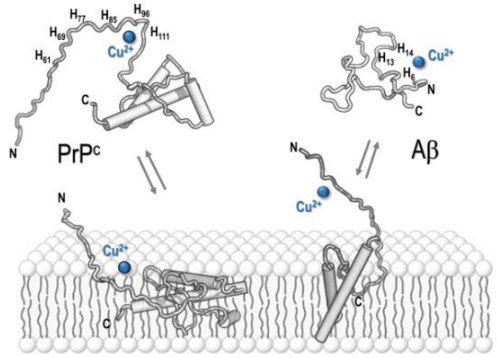

Scheme 1. Schematic representation of the binding equilibria of PrP^C and Aβ to membranes, showing the different position of the copper sites for the membrane-bound peptides, within the membrane for PrP^C and outside the membrane for Aβ.

Endogenous Peptide modifications. The capacity to generate ROS, and hence Cu redox cycling, by Cu^{II}-$Aβ_{40}$ in SDS micelles was recently reported,[37] although whether the peptide itself were affected by the oxidizing species was not investigated. In our experiments, we use catechols both as inducers of oxidative stress and as possible source of covalent modification of the peptide. Therefore, it is important to compare the oxidative and covalent modifications undergone by $Aβ_{40}$ in the aqueous and SDS environments. As we did before in the experiments of MC oxidation by Cu-Aβ complexes,[23c] we analyzed the modification of the peptide at various reaction times to assess if the reduced reactivity observed in SDS was accompanied by a change in the peptide modification pattern. In these experiments, we had to resort to a preliminary extraction of the organic phase, which interferes with the analysis of the peptide fragments by HPLC/MS. Unfortunately, this procedure did not enable to obtain reliable data in the case of Cu-$Aβ_{40}$ complexes, likely due to either aggregation and subsequent precipitation of $Aβ_{40}$ during the procedure or to extraction in the organic phase of this poorly hydrophilic peptide. The results obtained in the reactions carried out starting from Cu^{II}-Aβ and Cu^{I}-Aβ complexes (for $Aβ_{16}$ and $Aβ_{28}$) in SDS micelles are compared with those in aqueous buffer in Table 1 (MC) and 2 (DA).

Table 1. Percentage of unmodified Aβ peptides upon their reaction with MC in the presence of Cu^{II}, Cu^{II} and SDS micelles, or Cu^{I} and SDS micelles, in Hepes buffer pH 7.4 at 20 °C, as determined by LC/MS analysis.

	$Aβ_{16}$			$Aβ_{28}$			$Aβ_{40}$[a]
reaction time	**Cu^{II}**	**Cu^{II}/SDS**	**Cu^{I}/SDS**	**Cu^{II}**	**Cu^{II}/SDS**	**Cu^{I}/SDS**	**Cu^{II}**
30 min	65	91	96	62	77	82	50
90 min	35	80	83	21	62	70	41
180 min	25	60	68	8	35	62	32

[a] In the case of $Aβ_{40}$, we were unable to obtain reliable data on peptide modification by LC/MS analysis in experiments carried out in the presence of SDS micelles.

Table 2. Percentage of unmodified Aβ peptides upon their reaction with DA in the presence of Cu^{II}, or Cu^{II} and SDS micelles, in HEPES buffer pH 7.4 at 20 °C, as determined by LC/MS analysis.

	$Aβ_{16}$		$Aβ_{28}$		$Aβ_{40}$[a]
reaction time	**Cu^{II}**	**Cu^{II}/SDS**	**Cu^{II}**	**Cu^{II}/SDS**	**Cu^{II}**
30 min	73	81	87	88	65
90 min	65	70	64	76	58
180 min	52	58	37	64	52

[a] In the case of $Aβ_{40}$, we were unable to obtain reliable data on peptide modification by LC/MS analysis in experiments carried out in the presence of SDS micelles.

From the data in Tables 1 and 2, it is clear that SDS has a protective effect on $Aβ_{16}$ and $Aβ_{28}$ peptides. With MC, it is possible to appreciate that this effect is slightly more pronounced when the experiment is performed starting from Cu^{I} with respect to Cu^{II}; Aβ integrity starts to become appreciably affected after times of the order of half an hour. The derivatization of Aβ peptides promoted by Cu redox cycling and DA catalytic oxidation occurs at slower rate than in the case of MC oxidation, and the protective effect of SDS micelles becomes marked at long reaction times.

Regarding the type and sites of Aβ modification, histidines at positions 13 and 14 are the major sites undergoing O-atom insertion (mass increment +16 for each oxidized His, with a slight prevalence of oxidation at His14), and His6 the favored site for quinone addition (resulting in a His-catechol adduct, +122 for MC and +151 for DA, respectively) and quinone addition followed by oxidation of the catechol adduct (+120 and +149, for MC and DA, respectively), in line with previous observations (see Table S1, S3 and Figure S15, S17).[21b] Furthermore, in the DA promoted reaction we also considered the potential reactivity of indole-5,6-quinone (IQ) toward His residues. IQ derives from oxidation of 5,6-dihydroxyindole (DHI) that represents a rearrangement product of dopaminochrome, and its reactivity towards αSyn has been demonstrated.[43] Indeed, LC/MS analysis revealed the presence of His-DHI and His-IQ adducts (+147 and +145, respectively), albeit at low levels, with percent modifications comparable to those of His-DA and His-DAQ adducts (see Table S2, S4 and Figure S16, S18).

Overall, apart from the reduced fraction of modified peptide, the pattern of modifications is similar to those observed in aqueous medium, with one notable exception represented by the favored oxidation site in $Aβ_{28}$ that shifts from the histidines to Tyr10 in the presence of SDS. The more extensive analysis performed in the case of MC oxidation shows that the impact on the endogenous peptide appears to be essentially independent of whether the experiments are performed using Cu^{II} or Cu^{I} followed by exposure to air of the solution, apart from a slight reduction in reaction rate.

Besides oxidation and catechol/quinone adduct formation, in our reaction conditions, Aβ peptides are also susceptible to fragmentation, and this reaction appears to be more pronounced for $Aβ_{28}$ with respect to $Aβ_{16}$ and $Aβ_{40}$, with Asp1-Ala2 and His13-His14 as the preferred cleavage sites. It is noteworthy that the main targets of oxidative modifications and quinone additions are histidine residues (His13/His14 and His6, respectively) which are involved

in both Cu^{II} and Cu^{I} coordination by direct imidazole-metal bonds.[32b,44] Also the above reported sites of peptide fragmentation indicate the preferential reactivity of ROS generated by Cu-Aβ complexes towards targets located in proximity to the metal site. The consequent impairment of peptide structure will likely compromise the stability of Cu-Aβ complexes and their further redox reactivity.

As for Aβ peptides, also PrP_{76-114} was analyzed by LC/MS to characterize the oxidative and covalent modification undergone at long reaction times by the peptide in the presence of Cu^{II} and catechols, both in aqueous medium and membrane-like environment. Again, the high levels of unmodified peptide prove the protective effect exerted by SDS micelles on the peptide (Table 3). However, as the Cu-peptide complex is not tightly bound to the micelles the reactivity can be ascribed to a small fraction in equilibrium in the aqueous phase. It is also likely that the fraction undergoing oxidative modification is released from the SDS micelles. It is interesting that a difference in type of peptide modification can be noted between experiments carried out in water *vs.* SDS micelles. In fact, we found a prevalence of oxidation at His96 (and less at His85) in aqueous solution, but in the C-terminal region (i.e. at His111, Met109, or Met112) in the presence of SDS micelles. This means that the (main) targets of O-atom insertion belong to the coordination sphere of Cu^{II} (His85/His96) in water and to that of Cu^{I} (Met109/His111/Met112) in membrane-like environment, reflecting the metal species mainly involved in PrP complexation in the two phases. Regarding the modifications involving catechol residues, the amounts of His-DA/DAQ adducts are all detected at very low levels and His-DHI/IQ modifications are absent (see Table S6, S7 and Figure S20, S21).

Table 3. Percentage of unmodified PrP_{76-114} peptide upon its reaction with MC or DA in the presence of Cu^{II} or Cu^{II} and SDS micelles, in HEPES buffer pH 7.4 at 20 °C, as detected by LC/MS analysis.

	MC		**DA**	
reaction time	**Cu^{II}**	**Cu^{II}/SDS**	**Cu^{II}**	**Cu^{II}/SDS**
30 min	**66**	**79**	**81**	**86**
90 min	**57**	**71**	**75**	**84**
180 min	**19**	**67**	**61**	**73**

It is important to gain an appreciation of how efficient is the catalytic activity of the Cu-peptide complexes and how the modifications undergone by the peptide compete with catechol oxidation in the absence and presence of SDS. The oxidation of catechol during the reaction promoted by Cu^{II}-peptide complexes can be monitored performing the reaction in deuterated buffer through NMR (Figure S22), by analyzing samples withdrawn at various reaction times. Some selected data on turnover numbers of MC oxidation at various times and ratio of oxidized catechol vs. fraction of modified peptide, as deduced from Table 1 and 3, are collected in Table 4 (for a more extensive set of data on MC oxidation see Table S8 and S9, and Figure S23). The reactivity of Cu^{II}-Aβ complexes and Cu^{II}-PrP_{76-114} is similar, with the partial exception of Cu^{II}-$Aβ_{16}$, the reactivity of which it is slightly higher, probably due to the smaller size of the peptide, which may facilitate substrate binding and processing. Although in general the oxidation of catechol by Cu^{II}-peptide complexes is not particularly efficient, the reaction proceeds for hours, even though at decreasing rate with progress of time, because the peptide is partially damaged competitively. In this regard, we assume that oxidation, covalent modification (occurring especially at histidines), and cleavage of the peptide will weaken its copper binding properties and reduce the activity of the complex. The effect of quenching of the reaction in SDS is thus pronounced at short reaction times, but as the peptide is competitively modified, the resulting Cu-peptide fragments are released from the lipid phase and exhibit further reactivity, albeit with lower efficiency than the original Cu^{II}-peptide complexes.

Ternary Interaction between Cu^{II}, Aβ and PrP Peptides in SDS micelles. The interaction of prion protein with a variety of proteins appears to be involved in slowly and rapidly progressive forms of AD,[45] and in particular the interaction between cellular PrP and Aβ oligomers has been shown to mediate loss of synapses, aberrant signaling and cognitive decline in AD models.[46] We have thus tried to investigate whether $Aβ_{40}$ and PrP_{76-114} were able to interact, in aqueous buffer and/or in SDS micelles, and whether this condition. As discussed above, the two peptides are essentially unstructured in aqueous buffer, and as shown in Figure 6, combining $Aβ_{40}$ and PrP_{76-114} in 1:1 ratio does not produce any significant CD change attributable to ordered structures. However, the addition of slight sub-stoichiometric amount of Cu^{II} bears an appreciable reduction in the intensity in the CD peak near 200 nm, suggesting some local ordering of the peptides, that was not observed in the binary $Cu^{II}/Aβ_{40}$ and Cu^{II}/PrP_{76-114} binary systems (Figure 1 and S2). Some effect attributable to Cu^{II} can be noted also when the ternary system $Cu^{II}/Aβ_{40}/PrP_{76-114}$ is studied in SDS micelles. In this medium, $Aβ_{40}$ is partially structured and the α-helical portion of this peptide is the dominant feature of the CD spectrum when $Aβ_{40}$ and PrP_{76-114} are mixed in a 1:1 ratio (Figure 7). However, the further addition of sub-stoichiometric Cu^{II} produces a change in the relative intensity of the peaks at 208 and 222 nm, leading to an increased $[θ_{222}]/[θ_{208}]$ ellipticity ratio, which is not observed for the binary Cu^{II}-$Aβ_{40}$ complex (Figure 1C). Similar effects can be noted recording CD spectra for the $Cu^{II}/Aβ_{28}/PrP_{76-114}$ (Figure S24 and S25) and also $Cu^{II}/Aβ_{16}/PrP_{76-114}$ (Figure S26 and S27) ternary systems, suggesting that it is indeed the immediate copper(II) environment mainly responsible for the observed local structuring of the peptides.

In principle, in the absence of interaction between the two peptides, Cu^{II} should partition between $Aβ_{40}$ and PrP_{76-114} according to the relative affinity for them. The literature data on the affinity of Cu^{II} towards Aβ peptides shows a range of values, depending on the technique used.[47] For a better comparison with PrP_{76-114}, it is desirable to use data obtained with the same method. We can therefore assume for Cu^{II}-Aβ the log K value of 10.3 obtained for $Aβ_{16}$,[48] and for Cu^{II}-PrP_{76-114} log K = 14.3.[14b] Thus, in principle, in the absence of interaction between the peptides, the mixture of $Cu^{II}/Aβ_{40}/PrP_{76-114}$ should display dominant features of the Cu^{II}-PrP_{76-114} complex.

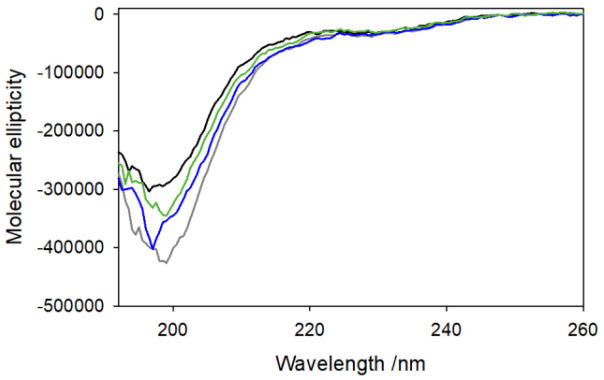

Figure 6. CD spectra recorded in 5 mM phosphate buffer solution pH 7.4 of $A\beta_{40}$ peptide (4.2 μM) (black spectrum) and after the addition of $PrP_{76\text{-}114}$ (4.2 μM) (grey), and then Cu^{II} (3.8 μM) (blue trace). The CD spectrum of the solution of Cu-$A\beta_{40}$-$PrP_{76\text{-}114}$ was recorded also after 2.5 h incubation time at 20 °C (green trace).

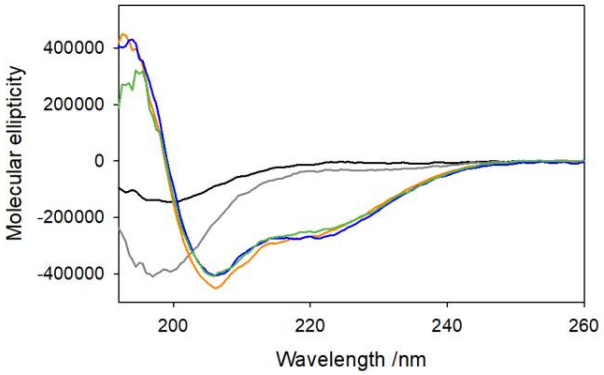

Figure 7. CD spectra recorded in 5 mM phosphate buffer solution pH 7.4 of $PrP_{76\text{-}114}$ (3.64 μM) (black spectrum) and after addition of $A\beta_{40}$ (3.64 μM) (grey), and SDS (20 mM) (orange). Then, Cu^{II} (3.31 μM) was added to the solution (blue) to generate the ternary complex Cu-$A\beta_{40}$-$PrP_{76\text{-}114}$. The CD spectrum of the solution of Cu-$A\beta_{40}$-$PrP_{76\text{-}114}$ was recorded also after 2.5 h incubation time at 20 °C (green trace).

We tried to obtain information about coordination of Cu^{II} in the ternary complex of Cu^{II}-Aβ40-$PrP_{76\text{-}114}$ by recording the CD spectrum in the near-UV and visible regions, and comparing it with those of the corresponding binary complexes. Already at a concentration of less than 0.1 mM the combination of Cu^{II}, $A\beta_{40}$, and $PrP_{76\text{-}114}$ yielded a precipitate in aqueous buffer, but the addition of SDS was able to at least partially dissolve it. The near-UV/visible CD spectrum of the ternary system in SDS micelles is shown in Figure S28. It is interesting that the CD features are different from the reported CD spectra of both Cu^{II}-Aβ[49] and Cu^{II}-$PrP_{76\text{-}114}$[14b] peptides throughout the entire spectral range. In particular, the CD peak in the range between 300 and 320 nm, due to amide-Cu^{II} LMCT,[49] has positive sign in the spectra of both binary complexes and is now negative in that of Cu^{II}-$A\beta_{40}$-$PrP_{76\text{-}114}$. The CD spectrum in Figure S28 is also different from that of a recently reported ternary complex of Cu^{II} with $A\beta_{16}$ and a small octarepeat PrP fragment (which also bears positive CD activity near 300 nm),[50] confirming that in Cu^{II}-$A\beta_{40}$-$PrP_{76\text{-}114}$, the copper ion is bound in the high affinity site outside the octarepeats.

Table 4. Selected comparative data on MC oxidation, turnover number (TON), and molar ratio of oxidized catechol vs. modified endogenous peptide, by Cu^{II}-peptide complexes, after 30 and 90 min reaction time, in aqueous buffer and in SDS micelles. Reaction conditions are: [MC] = 3 mM, [Cu-peptide] = 0.025 mM, in 50 mM HEPES buffer at pH 7.4 in the absence and presence of 20 mM SDS.

	30 min reaction time			**90 min reaction time**		
Complex	Δ[MC][a] (mM)	TON[b]	$\frac{\Delta[MC]}{\Delta[peptide]}$[b],[c]	Δ[MC][a] (mM)	TON[b]	$\frac{\Delta[MC]}{\Delta[peptide]}$[b],[c]
Buffer						
Cu^{II}-$A\beta_{16}$	0.33	13	38	0.61	24	37
Cu^{II}-$A\beta_{28}$	0.17	7	17	0.55	22	28
Cu^{II}-$A\beta_{40}$	0.21	8	18	0.48	19	32
Cu^{II}-$PrP_{76\text{-}114}$	0.20	8	24	0.67	27	62
SDS micelles						
Cu^{II}-$A\beta_{16}$	0.04	2	17	0.34	14	68
Cu^{II}-$A\beta_{28}$	0.06	2	10	0.20	8	21
Cu^{II}-$A\beta_{40}$	0.05	2	[d]	0.28	11	[d]
Cu^{II}-$PrP_{76\text{-}114}$	0.07	3	13	0.27	11	37

[a]Δ[MC] is concentration of oxidized MC. [b]Rounded to unity. [c]Δ[MC]/Δ[peptide] represents the ratio between the number of molecules of catechol oxidized *vs.* the fraction of endogenous peptide undergoing chemical modification at the given time. [d]Not available.

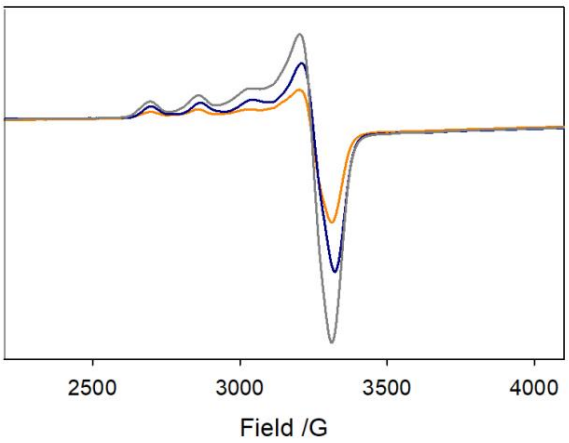

Figure 8. EPR spectra recorded in 5 mM phosphate buffer solution pH 7.4, containing 10% glycerol (v/v), for Cu^{II}-Aβ_{40} (~0.4 mM, orange spectrum) and upon the addition of PrP_{76-114} in 1:1 ratio (blue spectrum) and 19 mM SDS (grey). The signal amplitude was modified for better visualization.

Further information was obtained by EPR, upon freezing the solutions at low temperature. Figure 8 shows the spectrum of Cu^{II}-Aβ_{40} in 5 mM phosphate buffer, pH 7.4 (lower, orange trace), and the spectra obtained after addition of 1:1 PrP_{76-114} (intermediate, blue trace), and SDS (upper, grey trace). The EPR parameters calculated for Cu^{II}-Aβ_{40} ($g_{\|}$ = 2.28(0), $A_{\|}$ = 170×10^{-4} cm^{-1}, $g_{\perp}$ = 2.06) are in the range of values reported in the literature for a variety of Cu^{II} complexes with N-terminal Aβ fragments in various conditions,[51] and in particular are similar to those obtained for Cu^{II}-Aβ_{40} at pH 7.2 in highly saline medium.[52] Upon addition of PrP_{76-114} the EPR spectrum undergoes some detectable change, with parameters ($g_{\|}$ = 2.27(0), $A_{\|}$ = 179×10^{-4} cm^{-1}, $g_{\perp}$ = 2.06) more similar to those of Cu-PrP peptides.[14ab] The presence of SDS produces very slight change in the spectrum due to the modified environment ($g_{\|}$ = 2.27(7), $A_{\|}$ = 175×10^{-4} cm^{-1}, $g_{\perp}$ = 2.06). The EPR experiments then show that in the ternary complex, the Cu^{II} site is primarily within the PrP peptide, with the participation by Aβ_{40} in the primary coordination sphere that will need to be defined by further experiments.

Some further notable effects were noted studying DA oxidation by Cu^{II} in the presence of both Aβ_{40} and PrP_{76-114} (Figure 9B). Here, the reactivity of Cu-Aβ_{40}-PrP_{76-114} is higher than that of the individual Cu^{II}-Aβ_{40} and Cu^{II}-PrP_{76-114} complexes, while the addition of SDS quenches the reaction as before. The oxidation of MC shows a similar trend (Figure 9A). We notice that the increase in catechol oxidation rate in aqueous buffer is evident both in the initial fast phase (related to catechol oxidation and Cu^{II} reduction) and in the following catalytic turnover (involving a complex series of mechanistic events, the slow step probably connected with Cu^{I} reaction with O_2).[22,29] Similar increase in catechol oxidase activity was noted for the ternary Cu^{II}-Aβ_{28}-PrP_{76-114} and Cu^{II}-Aβ_{16}-PrP_{76-114} systems (Figure S29 and S30). The increased reactivity of the ternary Cu^{II}-Aβ-PrP_{76-114} complexes may be ascribed to easier redox cycling of Cu in the PrP site. Possibly, Aβ provides a histidine ligand preventing reduced copper to fall into the PrP site of low oxygen affinity comprised within the methionines. A possible arrangement of the Cu^{II} coordination set in the ternary Cu^{II}-Aβ-PrP_{76-114} complex is represented in Scheme 2.

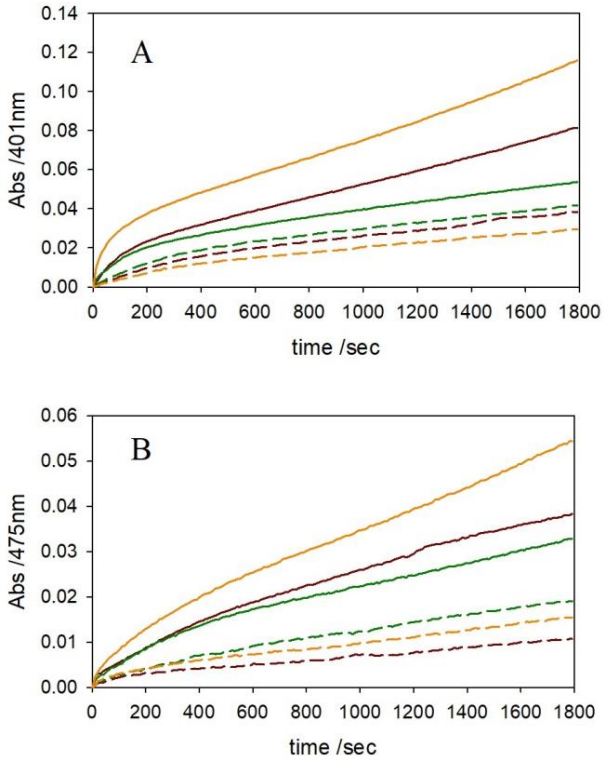

Figure 9. Kinetic profile of: (A) MC (3 mM) and (B) DA (3 mM) oxidation with time in 50 mM HEPES buffer solution at pH 7.4 and 20 °C. The oxidation of the substrates was performed: (i) in the presence of Cu^{II}-Aβ_{40} (25 μM) without (green solid line) and with SDS (20 mM, green dashed line); (ii) in the presence of Cu^{II}-PrP_{76-114} (25 μM) without (brown solid line) and with SDS (20 mM, brown dashed line); (iii) in the presence of Cu-Aβ_{40}-PrP_{76-114} (25 μM) without (orange solid line) and with SDS (20 mM, orange dashed line).

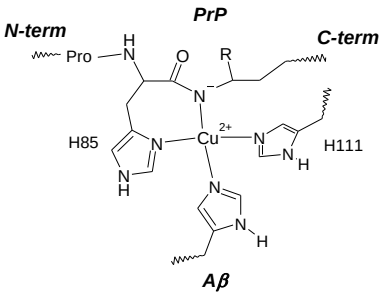

Scheme 2. Representation of the possible changes in the copper(II) coordination sphere in the ternary complex of Cu-Aβ_{40}-PrP_{76-114}. Numbering refer to the histidines in the PrP sequence.

BIOLOGICAL RELEVANCE AND CONCLUSIONS

The chemistry investigated here is promoted by the combination of three partners, a neuronal peptide, DA, and copper(II), which are prone to give an interaction favoring DA oxidation, since the peptides bear strong copper binding properties,[6,29] and the catechol group of DA is also a strong binding

ligand.[53] It is likely that in biological membranes this interaction will be stronger as the peptides contain fragments exhibiting high membrane affinity, anchoring them to the lipid moiety. The catecholamine itself has been shown to interact weakly with the surface of anionic phospholipid bilayers, with the cationic amino group serving as membrane anchoring site.[54] Thus, the redox chemistry induced by interaction of DA to Cu^{II}-bound peptides occurs across the surface of membranes, with stronger influence of the membrane-bound fraction as the Cu^{II}-peptide is entrapped in the lipid phase. The key event determining the quenching of Cu redox reactivity is the stabilization of the copper(I) species in the membrane.

In this regard, we should extend the results obtained for Cu-PrP and Cu-Aβ complexes to the previously studied Cu-αSyn complex.[23c] It is apparent that the DA-induced redox reactivity is blocked only for Cu-PrP and Cu-αSyn. Both latter peptides contain a couple of close methionines in the sequence, ^{109}MKHM^{112} in PrP[22,33] and ^{1}MDVFM^{5} in αSyn,[23c,55] that act as ligands stabilizing the Cu^{I} forms making them unreactive to dioxygen. For Cu^{I}-PrP_{76-114}, where the two Met residues are in the somewhat less favorable *i* and *i*+3 positions, metal binding is enforced by His111, between the two methionines.[33,39]

Previous studies on the reduction potential and redox cycling of Cu^{II}-PrP peptide complexes failed to unveil the key role of the methionines because the PrP sequences studied did not include these residues.[56] In any case, for both Cu^{I}-PrP^{76-114} and Cu^{I}-αSyn, the metal binding portion of the peptide is enclosed in the lipid phase (considering the relevant N-acetylated form of αSyn present in vivo). Thus, the two important features of PrP, as a strong Cu^{II} binding protein and as a neuroprotective agent preventing ROS production,[57] can be reconciled only if Cu^{II}-PrP remains bound to a membrane. Fragments of PrP resulting from e.g. cleavage by α-secretase,[58] and released in extracellular milieu are, instead, likely to be toxic because binding to Cu^{II} will induce redox reactivity.

The situation is different for Cu-Aβ complexes, where the binding site for both Cu^{II} and Cu^{I} is in the N-terminal, and polar portion of the peptide that remains essentially outside of the membrane. The reactivity of Cu-Aβ complexes decreases in SDS because a significant fraction of the substrate may stick on the micelle surface hindering its binding to the Cu center in the aqueous phase. It is known that DA prevents aggregation of $Aβ_{40}$,[28] but the effect was attributed only to oxidation of the peptide, essentially at Met35. The situation is quite certainly more complex, because it is likely that the main factor is the covalent peptide modification by a variety of DA derived quinone species, as it has been elucidated here (see Table S5 and Figure S19). This process is similar to the early steps of the biosynthesis of neuromelanins by reaction of oxidized catecholamines with peptides and proteins in several brain areas.[29] With the failure, or modest efficacy, of clinical trials with drugs promoting dissolution of amyloid deposits,[59,60] other sceneries must be envisaged. It is worth noting that experiments with transgenic mice models of AD showed intracellular Aβ immunoreactivity before cognitive loss and extensive amyloid plaques deposition.[61] Neurotransmitter reactivity and metal-induced oxidative stress are potential players in these early events involving aberrant Aβ modifications.

Regarding the last point, we wish to emphasize that in addition to the extensive evidence that the interaction of cellular PrP with Aβ oligomers plays some important role in the impairment of signaling pathways, synapse loss, and cognitive decline in several AD models,[62] Aβ neurotoxicity has been also connected to the interaction between monomeric Aβ, PrP and copper(II), which causes dysfunctions at N-methyl-D-aspartate receptors.[15] In this case, Aβ will likely be involved in a ternary complex mimicked by the Cu-$Aβ_{40}$-PrP_{76-114} species studied here. This complex is stabilized and redox silenced in SDS micelles but exhibits increased reactivity against DA in aqueous solution. We are strongly committed to perform a more thorough characterization of this key ternary complex employing NMR and other techniques to define the copper binding residues and understand the nature of the interaction between the two peptides, besides their eventual assembly through coordination to the metal center.

EXPERIMENTAL SECTION

Peptide synthesis and purification. The synthesis of peptides PrP_{76-114} (Ac-^{76}PHGGGWGQPHGGWGQGGGTHSQWNKPSKPKTNMKHMAG^{114}-NH_2, mw 4074.5), $PrP_{106-114}$ (Ac-^{106}KTNMKHMAG^{114}-NH_2, mw 1057.5),[22] $Aβ_{16}$ (1DAEFRHDSGYEVHHNK16-NH2, mw 1955.0), and $Aβ_{28}$ (^{1}DAEFRHDSGYEVHHNKLVFFAEDVGSNK^{28}-NH_2, mw 3262.5) is reported elsewhere.[21b] The purified peptides were lyophilized and stored at -20 °C until use. $Aβ_{40}$ (^{1}DAEFRHDSGYEVHHQKLVFFAEDVGSNKGAIIGLMVGGVV^{40}, mw 4329.8) was purchased from Eurogentec (Liège, Belgium). The purity of all peptides was >95% For the preparation of solutions of $Aβ_{40}$, the peptide was treated with hexafluoroisopropanol (HFIP) and incubated at room temperature for 3 h. Lyophilized peptide was then dissolved in water containing 0.6 mM NH_3 to prevent amyloid aggregation.[42]Blank experiments showed that the addition of NH_3 to Cu^{II}-Aβ complexes does not alter the rate of oxidation of catechols or the oxidative peptide modifications.

Effect of SDS and Cu on the secondary structure of peptides monitored by CD. The far-UV CD spectrum of Cu^{II}-PrP_{76-114} in 5 mM phosphate buffer solution at pH 7.4 (Figure S1 and S2) was recorded with a 0.1 cm path-length cell, while a cell of 1 cm path length was used for all other spectra. The CD data of Cu^{I}-peptide complexes were obtained in anaerobic conditions using 1 cm path-length cells with Schlenk connections. For Cu^{II}-PrP_{76-114}, the effect of increasing concentration of SDS (from 0 to 20 mM) was studied upon adding Cu^{II} (1 equiv.) to the solution of PrP_{76-114} (1.1 equiv.). To study the effect of SDS, the CD spectra of $Aβ_{28}$, $Aβ_{40}$ and PrP_{76-114} (1.1 equiv.) in the presence of Cu^{I} (1 equiv.) were initially recorded in 5 mM phosphate buffer solution pH 7.4, and then after the addition of SDS (20 mM). Cu^{I} was generated by reduction of copper(II) nitrate (1 equiv.) by hydroxylamine (2 equiv.) anaerobically. In the case of $Aβ_{40}$, Cu^{I} was re-oxidized to Cu^{II} through O_2 saturation. CD measurements were routinely carried out with scanning rate of 50 nm/min and 10 accumulations. The CD spectra of ternary complexes were obtained upon addition of PrP_{76-114} (1.1 equiv.) to a solution of 1.1 equiv. of Aβ fragments ($Aβ_{40}$, $Aβ_{28}$, or $Aβ_{16}$) in 5 mM phosphate buffer solution pH 7.4, followed maintained to record the CD spectra of ternary complexes in SDS: PrP_{76-114} (1.1 equiv.) was added to a solution of Aβ fragments ($Aβ_{40}$, $Aβ_{28}$, or $Aβ_{16}$, 1.1 equiv.), followed by SDS (20 mM), and Cu^{II} (1

equiv.). Optical spectra of solutions with the same ratio between $A\beta_{40}$/PrP_{76-114} and Cu^{II} were recorded using a 1 cm path-length cell for the near-UV and 10 cm cell for the visible region.

Catalytic oxidation of MC by Cu^{II}, [Cu^{II}-PrP] and [Cu^{II}-Aβ] complexes, in the presence of SDS. The catalytic oxidation of MC by Cu^{II} complexes was studied at 20 °C in 50 mM HEPES buffer at pH 7.4, saturated with atmospheric oxygen. The reaction was monitored by UV-visible spectroscopy following the 4-methyl-quinone band at 401 nm (ε = 1550 $M^{-1}cm^{-1}$) for a reaction time of 1800 s. The concentration of substrate was kept constant at 3 mM. The concentration of the peptides ($A\beta_{16}$, $A\beta_{28}$, $A\beta_{40}$, $PrP_{106-114}$, and PrP_{76-114}) was generally 50 μM, and that of copper(II) nitrate 25 μM unless otherwise stated. In the experiment with excess $PrP_{106-114}$, the peptide was added at 250 μM concentration to the solution of MC (3 mM), followed by copper(II) nitrate (25 μM) as the last reagent. The kinetic behavior of Cu^{II}-peptide complexes in presence of variable amounts of SDS (0-20 mM) was studied in the same conditions. The catalytic activity of the ternary complex Cu^{II}-$A\beta_{40}$-PrP_{76-114} (25 μM) was studied with and without SDS (20 mM). Blank experiments of MC autoxidation, in the absence of Cu^{II}, were carried out and the corresponding absorption was subsequently subtracted from the kinetic profiles. All measurements were performed at least in duplicate.

Catalytic oxidation of MC by Cu^{I}, [Cu^{I}-PrP] and [Cu^{I}-Aβ] complexes and O_2 in the presence of SDS. To study the oxidation of MC starting from an anaerobic solution of cuprous ions, Cu^{I} was generated in situ by reaction of copper(II) nitrate (25 μM) and ascorbate (50 μM) in the presence of SDS (20 mM), in deaerated 50 mM HEPES buffer a pH 7.4. Then, MC (3 mM) was added and the solution was rapidly exposed to air. As before, the oxidation of substrate was monitored by UV-visible spectroscopy through the growth of the 4-methyl-quinone band at 401 nm. The same experiment was repeated in the presence of Cu^{I}-peptide complexes ($A\beta_{16}$, $A\beta_{28}$, $A\beta_{40}$, $PrP_{106-114}$, and PrP_{76-114}) using peptide concentration of 50 μM. The kinetic traces were influenced by oxygen diffusion and whole consumption of ascorbate. All measurements were performed at least in duplicate.

Catalytic oxidation of DA by Cu^{II}, [Cu^{II}-PrP] and [Cu^{II}-Aβ] complexes in the presence of SDS. The catalytic oxidation of DA by Cu^{II} was studied at 20 °C in 50 mM HEPES buffer at pH 7.4, saturated with atmospheric oxygen. The reaction was monitored by UV-visible spectroscopy through the development of dopaminochrome band at 475 nm. The experiments were carried out by adding copper(II) nitrate (25 μM) to the solution containing DA (3 mM), in absence and in presence of SDS (20 mM), and adding each of the following peptides (50 μM): $A\beta_{16}$, $A\beta_{28}$, $A\beta_{40}$, PrP_{76-114} and $PrP_{106-114}$. The reactions catalyzed by ternary Cu^{II}-PrP_{76-114}-Aβ species were studied by the addition of 1 equiv. of PrP and $A\beta_{16}$/$A\beta_{28}$/$A\beta_{40}$ peptides (25 μM) to the reaction solution with and without SDS (20 mM). Copper(II) (25 μM) was added at the last reagent. DA (3 mM) autoxidation was also recorded in the same conditions. All measurements were performed at least in duplicate.

Identification and characterization of modified peptides from catechol oxidation experiments in the presence of SDS by HPLC-ESI/MS. The competitive peptide modification was studied by HPLC-ESI/MS, performing experiments in the same conditions used for kinetic studies. Samples were prepared in the following conditions: Cu^{II} (25 μM) or Cu^{I} (25 μM), the peptide ($A\beta_{16}$, $A\beta_{28}$, $A\beta_{40}$, or PrP_{76-114}) (50 μM), MC (3 mM), in the absence and presence of SDS (20 mM) in 50 mM HEPES buffer pH 7.4. Copper(I) was generated as described above. Sulfuric acid was added to quench the reaction (to pH~2) at different reaction times. Before LC-MS/MS analysis, SDS was precipitated by the addition of excess KCl. After standing for 2 h in ice, samples were centrifuged for 2 min. The supernatant was further left in ice for 30 min and centrifuged for 2 min in order to minimize the SDS content. The experiments of peptide modifications were also studied for DA (3 mM) oxidation reactions by Cu^{II} (25 μM), in the absence and presence of SDS (20 mM), with each one of the above peptides. Quenching of the reactions and SDS elimination was performed as described for reactions with MC. The elution of the mixtures for LC-MS/MS analysis was carried out by using 0.1% HCOOH in distilled water (solvent A) and 0.1% HCOOH in acetonitrile (solvent B), with a flow rate of 0.2 mL/min. Elution started with 98% solvent A for 5 min followed by a linear gradient from 98 to 55% A in 65 min. In the case of $A\beta_{40}$ samples, elution conditions were optimized with a linear gradient from 98 to 0% A in 65 min.

NMR quantification of oxidized catechol. The consumption of MC through ^{1}H-NMR spectroscopy was monitored as reported before.[22] The spectra of reaction solutions containing MC were recorded in 5 mM deuterated HEPES buffer at pH 7.4 (uncorrected for isotope effect) and 20 °C. In the case of MC (3 mM), the reaction started upon addition of copper(II) nitrate (25 μM), in the absence or presence of SDS (20 mM), for each the peptide fragments $A\beta_{16}$, $A\beta_{28}$, $A\beta_{40}$, and PrP_{76-144} (25 μM). The initial data were obtained after 5 min, which is the time required to acquire a reliable spectrum. The acquisition was repeated in the same conditions every 30 min until 150 min reaction time. In order to overcome the low availability of dioxygen in the NMR tube, the reactions were carried out in an open vial and samples were transferred to the NMR tube prior to each spectral recording. A blank experiment performed entirely in the NMR tube confirmed that the reaction rate of MC oxidation was much slower due to slow diffusion of dioxygen to replace its consumption in the solution. All measurements were performed at least in duplicate.

ASSOCIATED CONTENT

Supporting Information. CD spectra, ^{1}H-NMR spectra and related tables, HPLC/ESI-MS chromatograms and related tables, and plots of catechol oxidation. This material is available free of charge via the Internet at http://pubs.acs.org.

AUTHOR INFORMATION

Corresponding Authors

* enrico.monzani@unipv.it.

* luigi.casella@unipv.it.

ORCID id

Chiara Bacchella: 0000-0003-3256-8699

Stefania Nicolis: 0000-0002-6618-7555

Simone Dell'Acqua: 0000-0002-1231-4045
Enrico Monzani: 0000-0002-8791-6446
Enrico Rizzarelli: 0000-0001-5367-0823
Luigi Casella: 0000-0002-7671-0506

Author Contributions

C.B. synthesized the peptides and performed spectral and HPLC/MS analyses and catechol oxidation experiments. S.N. contributed to analyses of HLPC/MS data. S.D. contributed to spectroscopic analyses and analysis of kinetic studies. E.M. and L.C. conceived the project. E.R., E.M. and L.C. prepared the manuscript.

Funding Sources

Italian Ministry of Education, University, and Research (MIUR) - Research Projects of National Interest (PRIN) 2015 prot. 2015T778JW.

Notes

The authors declare no competing financial interest.

ACKNOWLEDGMENT

The authors acknowledge the Italian Ministry of Education, University, and Research (MIUR) - Research Projects of National Interest (PRIN) 2015 prot. 2015T778JW. C.I.R.C.M.S.B. is also acknowledged. We also thank prof. Daniele Dondi, University of Pavia, for recording the EPR spectra.

REFERENCES

1. (a) Greenough, M. A.; Camakaris, J.; Bush, A. I. Metal dyshomeostasis and oxidative stress in Alzheimer's disease. *Neurochem. Int.* **2013,** *62,* 540-555; (b) Kepp, K. P. Alzheimer's disease: How metal ions define β-amyloid function. *Coord. Chem Rev.* **2017**, *351,* 127-159; (c) Carboni, E.; Lingor, P. Insights on the interaction of alpha-synuclein and metals in the pathophysiology of Parkinson's disease. *Metallomics* **2015**, *7,* 395-404; (d) Faller, P.; Hureau, C.; Barthomieu, O. Role of Metal Ions in the Self-assembly of the Alzheimer's Amyloid-β Peptide. *Inorg. Chem.* **2013**, *52,* 12193-12206.

2. Mizuno, D.; Kawahara, M. Link between metal homeostasis and neurodegenerative diseases: Crosstalk of metals and amyloidogenic proteins at the synapse. In *Metallomics: recent analytical techniques and applications*; Ogra, Y.; Hirata, T., Eds.; Springer, 2017; pp. 285-314.

3. (a) Zecca, L.; Youdim, M. B.; Riederer, P.; Connor, J. R., Crichton, R. R. Iron, brain ageing and neurodegenerative disorders. *Nat. Rev. Neurosci.* **2004**, *5,* 863-873; (b) Zucca, F. A.; Cupaioli, F.A. Zecca, L. The role of iron in neurodegeneration. In *Neurodegeneration: metallostasis and proteostasis;* Milardi, D.; Rizzarelli, E., Eds.; RSC Publishing: Cambridge, 2011; pp. 174-211; (c) Zucca, F. A.; Segura-Aguilar, J.; Ferrari, E.; Muñoz, P.; Paris, I.; Sulzer, D.; Sarna, T.; Casella, L.; Zecca, L. Interactions of iron, dopamine and neuromelanin pathways in brain aging and Parkinson's disease. *Prog. Neurobiol.* **2017,** *155,* 96-119.

4. (a) Meiser, J.; Weindl, D.; Hiller, K. Complexity of dopamine metabolism. *Cell Communication and Signaling* **2013,** *11*:34 (doi:10.1186/1478-811X-11-34); (b) Segura-Aguilar, J.; Paris, I.; Muñoz, P.; Ferrari, E.; Zecca, L.; Zucca, F. A. Protective and toxic roles of dopamine in Parkinson's disease. *J. Neurochem.* **2014,** *129,* 898-915; (c) Herrera, A.; Muñoz, P.; Steinbusch, H. W. M.; Segura-Aguilar, J. Are dopamine oxidation metabolites involved in the loss of dopaminergic neurons in the nigrostriatal system in Parkinson's disease? *ACS Chem. Neurosci.* **2017,** *8,* 702−711.

5. Chang, C. J. Bioinorganic life and neural activity: toward a chemistry of consciousness? *Acc. Chem Res.* **2017,** *50,* 535-538.

6. Kawahara, M.; Kato-Negishi, M.; Tanaka, K. Cross talk between neurometals and amyloidogenic proteins at the synapse and the pathogenesis of neurodegenerative diseases. *Metallomics* **2017,** *9,* 619-633.

7. D'Ambrosi, N.; Rossi, L. Copper at synapse: Release, binding and modulation of neurotransmission. *Neurochem. Int.* **2015,** *90,* 30-45.

8. Ke, P. C.; Sani, M.-A.; Ding, F.; Kakinen, A.; Javed, I.; Separovic, F.; Davis, T. P.; Mezzenga, R. Implications of peptide assemblies in amyloid diseases. *Chem. Soc. Rev.* **2017,** *46,* 6492-6531.

9. (a) Aulic, S.; Masperone, L.; Narkiewicz, J.; Isopi, E.; Bistaffa, E.; Ambrosetti, E.; Pastore, B.; De Cecco, E.; Scaini, D.; Zago, P.; Moda, F.; Tagliavini, F.; Legname, G. α-Synuclein amyloids hijack prion protein to gain cell entry, facilitate cell-to-cell spreading and block prion replication. *Sci. Rep.* **2017,** *7,* 10050 (doi: 10.1038/s41598-017-10236-x); (b) Ferreira, D. G.; Temido-Ferreira, M.; Miranda, H. V.; Batalha, V. L.; Coelho, J. E.; Szego, E. M.; Marques-Morgado, I.; Vaz, S. H.; Rhee, J. S.; Schmitz, M.; Zerr, I.; Lopes, L. V.; Outeiro, T. F. α-synuclein interacts with PrP^C to induce cognitive impairment through mGluR5 and NMDAR2B. *Nat. Neurosci.* **2017,** *20,* 1569-1579; (c) Urrea, L.; Segura-Feliu, M.; Masuda-Suzukake, M.; Hervera, A.; Pedraz, L.; Aznar, J. M.; Vila, M.; Samitier, J.; Torrents, E.; Ferrer, I.; Gavin, R.; Hagesawa, M.; Del Rio, J. A. Involvement of cellular prion protein in α-synuclein transport in neurons. *Mol. Neurobiol.* **2018**, *55,* 1847-1860.

10. (a) Dohler, F.; Sepulveda-Falla, D.; Krasemann, S.; Altmeppen, H.; Schluter, H.; Hildebrand, D.; Zerr, I.; Matschke, J.; Glatzel, M. High molecular mass assemblies of amyloid-β oligomers bind prion protein in patients with Alzheimer's disease. *Brain* **2014**, *137,* 873-886. (b) Ganzinger, K. A. Narayan, P.; Qamar, S. S.; Weimann, L.; Ranasinghe, R. T.; Aguzzi, A.; Dobson, C. M.; McColl, J.; St George-Hyslop, P.; Klenerman, D. Single-molecule imaging reveals that small amyloid-β1–42 oligomers Interact with the cellular prion protein (PrP^C). *ChemBioChem* **2014,** *15,* 2515-2521; (c) Fluharty, B. R.; Biasini, E.; Stravalaci, M.; Sclip, A.; Diomede, L.; Balducci, C.; La Vitola, P.; Messa, M.; Colombo, L.; Forloni, G.; Borsello, T.; Gobbi, M.; Harris, D. A. An N-terminal fragment of the prion protein binds to amyloid-β oligomers and inhibits their neurotoxicity in vivo. *J. Biol. Chem.* **2013**, *288,* 7857-7866.

11. Wang, X. F.; Dong, C. F.; Zhang, J.; Wan, Y. Z.; Li, F.; Huang, Y. X.; Han, L.; Shan, B.; Gao, C.; Han, J.; Dong, X. P. Human tau protein forms complex with PrP and some GSS- and fCJD-related PrP mutants possess stronger binding activities with tau in vitro. *Mol. Cell. Biochem.* **2008,** *310,* 49-55.

12. (a) Costanzo, M.; Zurzolo, C. The cell biology of prion-like spread of protein aggregates: mechanisms and implication in neurodegeneration. *Biochem. J.* **2013,** 452, 1-17; (b) Brundin, P.; Melki, R.; Kopito, R. Prion-like transmission of protein aggregates in neurodegenerative diseases. *Nature Rev. Mol. Cell Biol.* **2010,** 11, 301–307; (c) del Río, J. A.; Ferrer, I.; Gavín, R. Role of cellular prion protein in interneuronal amyloid transmission. *Progr. Neurobiol.* **2018,** 165-167, 87-102.

13. (a) Laurén, J.; Gimbel D. A.; Nygaard, H. B.; Gilbert, J. W.; Strittmatter, S. M. Cellular prion protein mediates impairment of synaptic plasticity by amyloid-beta oligomers. *Nature* **2009**, *457,* 1128-1132; (b) Resenberger, U. K.; Winklhofer, K. F.; Tatzelt, J. Cellular prion protein mediates toxic signaling of amyloid beta. *Neurodegener. Dis.* **2012**, *10,* 298-300.

14. (a) Osz, K.; Nagy, Z.; Pappalardo, G.; Di Natale, G.; Sanna, D.; Micera, G.; Rizzarelli, E.; Sóvágó, I. Copper(II) interaction with prion peptide fragments encompassing histidine residues within and outside the octarepeat domain: Speciation, stability constants and binding details. *Chem. Eur. J.* **2007**, *13,* 7129-7143; (b) Di Natale, G.; Osz, K.; Nagy, Z.; Sanna, D.; Micera, G.; Pappalardo, G.; Sóvágó, I.; Rizzarelli, E. Interaction of copper(II) with the prion peptide fragment HuPrP(76–114) encompassing four histidyl residues within and outside the octarepeat domain. *Inorg. Chem.* **2009**, *48,* 4239-4250; (c) Di Natale, G.; Turi, I.; Pappalardo, G.; Sóvágó, I.; Rizzarelli, E. Cross-talk between the octarepeat domain and the fifth binding

site of prion protein driven by the interaction of copper(II) with the N-terminus. *Chem. Eur. J.* **2015,** *21,* 4071-4084; (d) Quintanar, L.; Rovillas-Acevedo, L.; Grande-Aztazi, R.; Gomez-Castro, C. Z.; Arcos-Lopez, T.; Vela, A. Copper coordination to the prion protein: Insights from theoretical studies. *Coord. Chem. Rev.* **2013**, *257*, 429-444.

15. You, H.; Tsutsui, S.; Hameed, S.; Kannanayakal, T. J.; Chen, L.; Xia, P.; Engbers, J. D. T.; Lipton, S. A.; Stys, P. K.; Zamponi, G. W. Aβ neurotoxicity depends on interactions between copper ions, prion protein, and N-methyl-d-aspartate receptors. *Proc Natl. Acad. Sci.* **2012,** *109,* 1737-1742.

16. Chen, S. G.; Teplow, D. B.; Parchi, P.; Teller, J. K.; Gambetti, P.; Autilio-Gambetti, L. Truncated forms of the human prion protein in normal brain and in prion diseases. *J. Biol. Chem.* **1995,** *270,* 19173-19180.

17. McDonald, A. J.; Dibble, J. P.; Evans, E. G. B.; Millhauser, G. L. A new paradigm for enzymatic control of α-cleavage and β-cleavage of the prion protein. *J. Biol. Chem.* **2014,** *289,* 803-813.

18. (a) Deas, E.; Cremades, N.; Angelova, P. R.; Ludtmann, M. H. R.; Yao, Z.; Chen, S.; Horrocks, M. H.; Banushi, B.; Little, D.; Devine, M. J.; Gissen, P.; Klenerman, D.; Dobson, C. M.; Wood, N. W.; Gandhi, S.; Abramov, A. Y. Alpha-synuclein oligomers interact with metal ions to induce oxidative stress and neuronal death in Parkinson's disease. *Antioxid. Redox Signal.* **2016,** *24,* 376-391; (b) Eskici, G.; Axelsen, P. H. Copper and oxidative stress in the pathogenesis of Alzheimer's disease. *Biochemistry* **2012,** *51,* 6289−6311; (c) Barnham, K. J.; Bush, A. I. Biological metals and metal-targeting compounds in major neurodegenerative diseases. *Chem. Soc. Rev.* **2014,** *43,* 6727-6743; (d) Valensin, D.; Dell'Acqua, S.; Kozlowski, H.; Casella, L. Coordination and redox properties of copper interaction with α-synuclein. *J. Inorg. Biochem.* **2016,** *163,* 292-300; (e) Kepp, K. P. Bioinorganic chemistry of Alzheimer's disease. *Chem. Rev.* **2012,** *112,* 5193-5239; (f) Faller, P.; Hureau, C.; La Penna, G. Metal ions and intrinsically disordered proteins and peptides: From Cu/Zn amyloid-β to general principles. *Acc. Chem. Res.* **2014,** *47,* 2252-2259.

19. (a) Gibson, G. E.; Huang, H.-M. Oxidative stress in Alzheimer's disease. *Neurobiol. Aging.* **2005,** *26,* 575–578; (b) Sultana, R.; Butterffield, D. A. Role of oxidative stress in the progression of Alzheimer's disease. *J. Alzheimers Dis.* **2010,** *19,* 341-353; (c) Zhang, J.; Perry, G.; Smith, M. A.; Robertson, D.; Olson, S. J.; Graham, D. G.; Montine, T. Parkinson's disease is associated with oxidative damage to cytoplasmic DNA and RNA in substantia nigra neurons. *Am. J. Pathol.* **1999,** *154,* 1423-1429; (d) Puspita, L.; Chung, S. Y.; Shim J.-W. Oxidative stress and cellular pathologies in Parkinson's disease. *Molecular Brain* **2017,** 10:53; (e) Hwang, O. Role of oxidative stress in Parkinson's disease. *Exp Neurobiol.* **2013**, 22, 11–17.

20. (a) Zou, K., Gong, J.-S., Yanagisawa, K., Michikawa, M. A novel function of monomeric amyloid β-protein serving as an antioxidant molecule against metal-induced oxidative damage. *J. Neurosci.* **2002,** *22,* 4833-4841; (b) Pedersen, J. T.; Chen, S. W.; Borg, C. B.; Ness, S.; Bahl, J. M.; Heegaard, N. H. H.; Dobson, C. M.; Hemmingsen, L.; Cremades, N.; Teilum, K. Amyloid-β and α-synuclein decrease the level of metal-catalyzed reactive oxygen species by radical scavenging and redox silencing. *J. Am. Chem. Soc.* **2016,** *138,* 3966-3969.

21. (a) Ciregna, D.; Monzani, E.; Thiabaud, G.; Pizzocaro, S.; Casella, L. Copper–β-amyloid peptides exhibit neither monooxygenase nor superoxide dismutase activities. *Chem. Commun.* **2013,** *49,* 4027-4029; (b) Pirota, V.; Dell'Acqua, S.; Monzani, E.; Nicolis, S.; Casella, L. Copper-Aβ peptides and oxidation of catecholic substrates: reactivity and endogenous peptide damage. *Chem. Eur. J.* **2016,** *22,* 16964-16973.

22. Dell'Acqua, S.; Bacchella, C.; Monzani, E.; Nicolis, S.; Di Natale, G.; Rizzarelli, E.; Casella, L. Prion peptides are extremely sensitive to copper induced oxidative stress. *Inorg. Chem.* **2017,** *56,* 11317-11325.

23. (a) Dell'Acqua, S.; Pirota, V.; Anzani, C.; Rocco, M. M.; Nicolis, S.; Valensin, D.; Monzani, E.; Casella, L. Reactivity of copper–α-synuclein peptide complexes relevant to Parkinson's disease. *Metallomics* **2015,** *7,* 1091-1102; (b) De Ricco, R.; Valensin, D.; Dell'Acqua, S.; Casella, L.; Hureau, C.; Faller, P. Copper(I/II), α/β-Synuclein and amyloid-β: Menage à trois? *ChemBioChem* **2015,** *16,* 2319-2328; (c) Dell'Acqua, S.; Pirota, V.; Monzani, E.; Camponeschi, F.; De Ricco, R.; Valensin, D.; Casella, L. Copper(I) Forms a redox-stable 1:2 complex with α-synuclein N-terminal peptide in a membrane-like environment. *Inorg. Chem.* **2016,** *55,* 6100-6106.

24. (a) Ostreova-Golts, N.; Petrucelli, L.; Hardy, J.; Lee, J. M.; Farer, M.; Wolozin, B. The A53T α-synuclein mutation increases iron-dependent aggregation and toxicity. *J. Neurosci.* **2000,** *20,* 6048-6054; (b) Cappai, R.; Leck, S.-L.; Tew, D. J.; Williamson, N. A.; Smith, D. P.; Galatis, D.; Sharpless, R. A.; Curtain, C. C.; Ali, F. E.; Cherry, R. A.; Culvenor, J. G.; Bottomley, S. P.; Masters, C. L.; Barnham, K. J.; Hill, A. F. Dopamine promotes alpha-synuclein aggregation into SDS-resistant soluble oligomers via a distinct folding pathway. *FASEB J.* **2005,** *19,* 1377-1379; (c) Plotegher, N.; Greggio, E.; Bisaglia M.; Bubacco, L. Biophysical groundwork as a hinge to unravel the biology of α-synuclein aggregation and toxicity. *Q. Rev. Biophys.* **2014,** *1,* 1–48.

25. (a) Spillantini, M. G.; Schmidt, M. L.; Lee, V. M.; Trojanowski, J. Q.; Jakes, R.; Goedert, M. Alpha-synuclein in Lewy bodies. *Nature* **1997,** *388,* 839-840; (b) Spillantini, M. G.; Crowther, R. A.; Jakes, R.; Hasegawa, M.; Goedert, M. α-Synuclein in filamentous inclusions of Lewy bodies from Parkinson's disease and dementia with Lewy bodies- *Proc. Natl. Acad. Sci. USA* **1998,** *95,* 6469-6473; Masliah, E.; Rockenstein, E.; Veinbergs, I.; Mallory, M.; Hashimoto, M.; Takeda, A.; Sagara, Y.; Sisk, A.; Mucke, L. Dopaminergic loss and inclusion body formation in α-synuclein mice: Implications for neurodegenerative disorders. *Science* **2000,** *287,* 1265-1269.

26. (a) da Luz, M. H. M.; Peres, I. T.; Santos, T. G.; Martins, V. R.; Icimoto, M. Y.; Lee, K. S. Dopamine induces the accumulation of insoluble prion protein and affects autophagic flux. *Front. Cel. Neurosci.* **2015,** *9,* 12; (b) Shiraishi, N.; Inai, Y.; Bi, W. M.; Nishikimi, M. Fragmentation and dimerization of copper-loaded prion protein by copper-catalysed oxidation. *Biochem. J.* **2005,** *387,* 247-255; (c) Rial, D.; Pamplona, F.A.; Moreira, E. L.; Moreira, K.M.; Hipolide, D.; Rodrigues, D. I.; Dombrowski, P. A.; Da Cunha, C.; Agostinho, P.; Takahashi, R. N.; Waltz, R.; Cunha, R. A.; Prediger, R. D. Cellular prion protein is present in dopaminergic neurons and modulates the dopaminergic system. *Eur. J. Neurosci.* **2014,** *40,* 2479-2484.

27. (a) Martorana, A.; Koch, G. "Is dopamine involved in Alzheimer's disease?" *Front. Aging Neurosci.* **2014,** *6,* 252; (b) Šimić, G.; Babić Lekoa, M.; Wray, S.; Harrington, C. R.; Delalle, I.; Jovanov-Milošević, N.; Bažadona, D.; Buée, L.; de Silva, R.; Di Giovanni, G.; Wischik, C. M.; Hof, P. R. Monoaminergic neuropathology in Alzheimer's disease. *Prog. Neurobiol.* **2017,** *151,* 101-138; (c) Nobili, A.; Latagliata, E. C.; Viscomi, M. T.; Cavallucci, V.; Cutuli, D.; Giacovazzo, G.; Krashia, P.; Rizzo, F. R.; Marino, R.; Federici, M.; De Bartolo, P.; Aversa, D.; Dell'Acqua, M. C.; Cordella, A.; Sancandi, M.; Keller, F.; Petrosini, L.; Puglisi-Allegra, S.; Mercuri, N. B.; Coccurello, R.; Berretta, N.; D'Amelio, M. Dopamine neuronal loss contributes to memory and reward dysfunction in a model of Alzheimer's disease. *Nat. Commun.* **2017,** *8,* 14727.

28. Nam, E.; Derrick, J. S.; Lee, S.; Kang, J.; Han, J.; Lee, S. J. C.; Chung, S. W.; Lim, M. H. Regulatory activities of dopamine and its derivatives toward metal-free and metal-induced amyloid-β aggregation, oxidative stress, and inflammation in Alzheimer's disease. *ACS Chem. Neurosci.* **2018,** *9,* 2655-2666.

29. Monzani, E.; Nicolis, S.; Dell'Acqua, S.; Capucciati, A.; Bacchella, C.; Zucca, F. A.; Mosharov, E. V.; Sulzer, D.; Zecca, L.; Casella, L. Dopamine, oxidative stress and protein–quinone modifications in Parkinson's and other neurodegenerative diseases. *Angew. Chem. Int. Ed.* **2019,** *58*, 6512–6527.

30. Zecca, L.; Stroppolo, A.; Gatti, A.; Tampellini, D.; Toscani, M.; Gallorini, M.; Giaveri, G.; Arosio, P.; Santambrogio, P.; Fariello, R. G.; Karatekin, E.; Kleinman, M. H.; Turro, N.; Hornikiewicz, O.; Zucca, F. A. The role of iron and copper molecules in the neuronal vulnerability of locus coeruleus and substantia nigra during aging. *Proc. Natl. Acad. Sci. USA* **2004,** *101,* 9843-9848.

31. (a) Boland, M. P.; Hatty, C. R.; Separovic, F.; Hill, A. F.; Tew, D. J.; Barnham, K. J.; Haigh, C. L.; James, M.; Masters, C. L.: Collins, S. J. Anionic phospholipid interactions of the prion protein N terminus are minimally perturbing and not driven solely by the octapeptide repeat domain. *J. Biol.*

Chem. **2010**, *285*, 32282-32292; (b) Lau, T.-L.; Ambroggio, E. E.; Tew, D. J.; Cappai, R.; Masters, C. L.; Fidelio, G. D.; Barnham, K. J.; Separovic, F. Amyloid-β peptide disruption of lipid membranes and the effect of metal ions. *J. Mol. Biol.* **2006,** *356*, 750-770; (c) Hecel, A.; De Ricco, R.; Valensin, D. Influence of membrane environments and copper ions on the structural features of amyloidogenic proteins correlated to neurodegeneration. *Coord. Chem. Rev.* **2016,** *327-328*, 8-19.

32. (a) Cheignon, C.; Jones, M.; Atrian-Blasco, E.; Kieffer, I.; Faller, P.; Collin, F.; Hureau, C. Identification of key structural features of the elusive Cu–Aβ complex that generates ROS in Alzheimer's disease. *Chem. Sci.* **2017,** *8*, 5107-5118; (b) Atrián-Blasco, E.; Gonzalez, P.; Santoro, A.; Alies, B.; Faller, P.; Hureau, C. Cu and Zn coordination to amyloid peptides: From fascinating chemistry to debated pathological relevance. *Coord. Chem. Rev.* **2018,** *371*, 38-55.

33. Arcos-Lopez, T.; Qayyum, M.; Rivillas-Acevedo, L.; Miotto, M. C.; Grande-Aztatzi, R.; Fernandez, C. O.; Hedman, B.; Hodgson, K. O.; Vela, A.; Solomon, E. I.; Quintanar, L. Spectroscopic and theoretical study of Cu^{I} binding to His111 in the human prion protein fragment 106–115. *Inorg. Chem.* **2016,** *55*, 2909-2922.

34. (a) Shearer, J.; Szalai, V. A. The amyloid-β peptide of Alzheimer's disease binds Cu^{I} in a linear bis-His coordination environment: Insight into a possible neuroprotective mechanism for the amyloid-β peptide. *J. Am. Chem. Soc.* **2008,** *130*, 17826-17835; (b) Himes, R. A.; Park, G. Y.; Siluvai, G. S.; Blackburn, N. J.; Karlin, K. D. Structural studies of copper(I) complexes of amyloid-β peptide fragments: Formation of two-coordinate bis(histidine) complexes. *Angew. Chem. Int. Ed.* **2008,** *47*, 9084–9087.

35. (a) Zhan, R.; Liu, A.; Luhrs, T.; Riek, R.; von Schoetter, C.; Lopez Garcia, F.; Billeter, M.; Calzolai, L.; Wider, G.; Wüthrich, K. NMR solution structure of the human prion protein. *Proc. Natl. Acad. Sci. USA* **2000,** *97*, 145-150; (b) Aguzzi, A.; Miele, G. Recent advances in prion biology. *Curr. Opin. Neurol.* **2004,** *17*, 337–342.

36. (a) Migliorini, C.; Sinicropi, A.; Kozlowski, H.; Luczkowski, M.; Valensin, D. Copper-induced structural propensities of the amyloidogenic region of human prion protein. *J. Biol. Inorg. Chem.* **2014,** *19*, 635–645; (b) Hecel, A.; Migliorini, C.; Valensin, D.; Luczkowski, M.; Kozlowski, H. Impact of SDS surfactant on the interactions of Cu^{2+} ions with the amyloidogenic region of human prion protein. *Dalton Trans.* **2015,** *44*, 13125-13132.

37. Tiiman, A.; Luo, J.; Wallin, C.; Olsson, L.; Lindgren, J.; Jarvet, J.; Ros, P.; Sholts, S. B.; Rahimipour, S.; Abrahams, J. P.; Karlström, A. E.; Gräslund, A.; Wärmländer, S. K. Specific binding of Cu(II) ions to amyloid-beta peptides bound to aggregation-inhibiting molecules or SDS micelles creates complexes that generate radical oxygen species. *J. Alzheimers Dis.* **2016,** *54*, 971-982.

38. (a) Coles, M.; Bicknell, W.; Watson, A. A.; Fairlie, D. P.; Craik, D. J. Solution structure of amyloid β-peptide(1–40) in a water–micelle environment. Is the membrane-spanning domain where we think it is? *Biochemistry* **1998,** *37*, 11064-11077; (b) Shao, H.; Jao, S.; Ma, K.; Zagorski, M. C. Solution structures of micelle-bound amyloid beta-(1-40) and beta-(1-42) peptides of Alzheimer's disease. *J. Mol. Biol.* **1999,** *285*, 755-773; (c) Gaggelli, E.; Janicka-Klos, A.; Jankowska, E.; Kozlowski, H.; Migliorini, C.; Molteni, E.; Valensin, D.; Valensin, G.; Wieczerzak, E. NMR studies of the Zn^{2+} interactions with rat and human β-amyloid (1–28) peptides in water-micelle environment. *J. Phys. Chem. B* **2008,** *112*, 100-109.

39. Sciacca, M. F. M.; Kotler, S. A.; Brender, J. R.; Chen, J.; Lee, D. K.; Ramamoorthy, A. Two-step mechanism of membrane disruption by Aβ through membrane fragmentation and pore formation. *Biophys. J.* **2012,** *103*, 702-710.

40. Ghalebani, L.; Wåhlström, A.; Danielsson, J.; Wärmländer, S. K.; Gräslund, A. pH-dependence of the specific binding of Cu(II) and Zn(II) ions to the amyloid-β peptide. *Biochem. Biophys. Res. Commun.* **2012,** *421*, 554-560.

41. (a) Herlinger, E.; Jameson, R. F.; Linert, W. Spontaneous autoxidation of dopamine. *J. Chem. Soc. Perkin Trans. 2* **1995,** *0*, 259-263 (1995); (b) d'Ischia, M.; Napolitano, A.; Ball, V.; Chen, C.-T.; Buehler, M. J. Polydopamine and eumelanin: from structure-property relationships to a unified tailoring strategy. *Acc. Chem. Res.* **2014,** *47*, 3541-3549.

42. Tougu, V.; Karafin, A.; Palumaa, P. Binding of zinc(II) and copper(II) to the full-length Alzheimer's amyloid-beta peptide. *J. Neurochem.* **2008,** *104*, 1249–1259.

43. Bisaglia, M.; Mammi, S.; Bubacco, L. Kinetic and structural analysis of the early oxidation products of dopamine: analysis of the interactions with alpha-synuclein. *J. Biol. Chem.* **2007,** *282*, 15597-15605.

44. Young, T. R.; Kirchner, A.; Wedd, A. G.; Xiao, Z. An integrated study of the affinities of the Aβ16 peptide for Cu(I) and Cu(II): implications for the catalytic production of reactive oxygen species. *Metallomics* **2014,** *6*, 505-517.

45. Zafar, S.; Shafiq, M.; Younas, N.; Schmitz, M.; Ferrer, I.; Zerr, I. Prion protein interactome: Identifying novel targets in slowly and rapidly progressive forms of Alzheimer's disease. *J. Alzheimers Dis.* **2017,** *59*, 265-275.

46. Lima-Filho, R. A. S.; Oliveira, M. M. A role for cellular prion protein in late-onset Alzheimer's disease: Evidence from preclinical studies. *J. Neurosci.* **2018,** *38*, 2146-2148.

47. Viles, J. H. Metal ions and amyloid fiber formation in neurodegenerative diseases. Copper, zinc and iron in Alzheimer's, Parkinson's and prion diseases. *Coord. Chem. Rev.* **2012,** *256*, 2271–2284; (b) Zawisza, I.; Rózga, M.; Bal, W. Affinity of copper and zinc ions to proteins and peptides related to neurodegenerative conditions (Aβ, APP, α-synuclein, PrP). *Coord. Chem. Rev.* **2012,** *256*, 2297–2307; (c) Conte-Daban, A.; Borghesani, V.; Sayen, S.; Guillon, E.; Journaux, Y.; Gontard, G.; Lisnard, L. Hureau, C. Link between affinity and Cu(II) binding sites to amyloid-β peptides evaluated by a new water-soluble UV–Visible ratiometric dye with a moderate Cu(II) affinity. *Anal. Chem.* **2017,** *89*, 2155–2162.

48. Damante, C. A.; Osz, K.; Nagy, Z.; Pappalardo, G.; Grasso, G.; Impellizzeri, G.; Rizzarelli, E.; Sovago, I., The metal loading ability of beta-amyloid N-terminus: a combined potentiometric and spectroscopic study of copper(II) complexes with beta-amyloid(1-16), its short or mutated peptide fragments, and its polyethylene glycol (PEG)-ylated analogue. *Inorg Chem* **2008,** *47* (20), 9669–9683.

49. Syme, C. D.; Nadal, R. C.; Rigby, S. E. J.; Viles, J. H. Copper binding to the amyloid-beta (Abeta) peptide associated with Alzheimer's disease: folding, coordination geometry, pH dependence, stoichiometry, and affinity of Abeta-(1-28): insights from a range of complementary spectroscopic techniques. *J. Biol. Chem.* **2004**, *279*, 18169-18177.

50. Magrì, A.; Di Natale, G.; Rizzarelli, E. Copper-assisted interaction between amyloid-β and prion: Ternary metal complexes with Aβ N-terminus and octarepeat. *Inorg. Chim. Acta* **2018**, *472*, 93-102.

51. (a) Drew, S. C.; Barnham, K. J. The heterogeneous nature of Cu^{2+} interactions with Alzheimer's amyloid-β peptide. *Acc. Chem. Res.* **2011**, *44*, 1146-1155; (b) Hureau, C.; Dorlet, P. Coordination of redox active metal ions to the amyloid precursor protein and to amyloid-β peptides involved in Alzheimer disease. Part 2: Dependence of Cu(II) binding sites with Aβ sequences. *Coord. Chem. Rev.* **2012**, *256*, 2175-2187.

52. Karr, J. W. Karr, Szalai, V. A. Cu(II) binding to monomeric, oligomeric, and fibrillar forms of Alzheimer's disease amyloid-β peptide. *Biochemistry* **2008**, *47*, 5006-5016.

53. Abd El Wahed, M. G.; Ayad, M. Stability constants of Cu^{2+}, $Fe^{3+}$and Zr^{4+} chelates of ampicillin, dopamine and α-methyl L-dopa in aqueous medium. *Anal. Letters* **1984,** *17*, 205-216.

54. Jodko-Piorecka, K.; Litwinienko, G. First experimental evidence of dopamine interactions with negatively charged model biomembranes. *ACS Chem. Neurosci.* **2013,** *4*, 1114-1122.

55. Miotto, M.; Valiente-Gabioud, A. A.; Rossetti, G.; Zweckstetter, M.; Carloni, P.; Selenko, P.; Griesinger, C.; Binolfi, A.; Fernandez, C. O. Copper binding to the N-terminally acetylated, naturally occurring form of alpha-synuclein induces local helical folding. *J. Am. Chem. Soc.* **2015**, *137*, 6444-6447.

56. Liu, L.; Jiang, D.; McDonald, A.; Hao, Y.; Millhauser, G. L.; Zhou, F. Copper redox cycling in the prion protein depends critically on binding mode. *J. Am. Chem. Soc.* **2011**, *133*, 12229-12237.

57. (a) Watt, N. T.; Routledge, M. N.; Wild, C. P.; Hooper, N. M. Cellular prion protein protects against reactive-oxygen-species-induced DNA damage. *Free Rad. Biol. Med.* **2007,** *43*, 959–967; (b) Biasini, E.; Turnbaugh, J. A.; Unterberger, U.; Harris, D. A. Prion protein at the crossroads of physiology and disease. *Trends Neurosci.* **2012,** *35*, 92–103.

58. Vincent, B.; Cisse, M. A.; Sunyach, C.; Guillot-Sestier, M. V.; Checler, F. Regulation of betaAPP and PrPc cleavage by alpha-secretase: mechanistic and therapeutic perspectives. *Curr. Alzheimer Res.* **2008,** *5*, 202-211.

59. Karran, E.; Hardy, J. Antiamyloid therapy for Alzheimer's disease – Are we on the right road? *New Engl. J. Med.* **2014,** *370*, 377–378.

60. Kepp, K. P. Alzheimer's disease due to loss of function: A new synthesis of the available data. *Prog. Neurobiol.* **2016,** *143*, 36-60.

61. Schmitz, C.; Rutten, B. P.; Pielen, A.; Schäfer, S.; Wirths, O.; Tremp, G.; Czech, C.; Blanchard, V.; Multhaup, G.; Rezaie, P., Korr, H.; Steinbusch, H. W.; Pradier, L.; Bayer, T. A. Hippocampal neuron loss exceeds amyloid plaque load in a transgenic mouse model of Alzheimer's disease. *Am. J. Pathol.* **2004**, *164*, 1495-1502.

62. (a) Lima-Filho, R. A. S.; Oliveira, M. M. A role for cellular prion protein in late-onset Alzheimer's disease: Evidence from preclinical studies. *J. Neurosci.* **2018**, *38*, 2146-2148; (b) Salazar, S. V.; Strittmatter, S. M. Cellular prion protein as a receptor for amyloid-β oligomers in Alzheimer's disease. *Biochem. Biophys. Res. Commun.* **2017**, *483*, 1143-1147; (c) Um, J. W.; Nygaard, H. B.; Heiss, J. K.; Kostylev, M. A.; Stagi, M.; Vortmeyer, A.; Wisniewski, T.; Gunther, E. C.; Strittmatter, S. M. Alzheimer amyloid-β oligomer bound to postsynaptic prion protein activates Fyn to impair neurons. *Nat. Neurosci.* **2012**, *15*, 1227-1235; (d) Um, J. W.; Kaufman, A. C.; Kostylev, M.; Heiss, J. K.; Stagi, M.; Takahashi, H.; Kerrisk, M. E.; Vortmeyer, A.; Wisniewski, T.; Koleske, A. J.; Gunther, E. C.; Nygaard, H. B.; Strittmatter, S. M. Metabotropic glutamate receptor 5 is a coreceptor for Alzheimer aβ oligomer bound to cellular prion protein. *Neuron* **2013**, *79*, 887-902; (e) Kostylev, M. A.; Kaufman, A. C.; Nygaard, H. B.; Patel, P.; Haas, L. T.; Gunther, E. C.; Vortmeyer, A.; Strittmatter, S. M. Prion-protein-interacting amyloid-β oligomers of high molecular weight are tightly correlated with memory impairment in multiple Alzheimer mouse models *J. Biol. Chem.* **2015**, *290*, 17415-17438.